Rupture models for the A.D. 900–930 Seattle fault earthquake from uplifted shorelines

Uri S. ten Brink
Jianli Song
U.S. Geological Survey, Woods Hole, Massachusetts 02543, USA
Robert C. Bucknam
U.S. Geological Survey, Golden, Colorado 80225, USA

ABSTRACT

A major earthquake on the Seattle fault, Washington, ca. A.D. 900–930 was first inferred from uplifted shorelines and tsunami deposits. Despite follow-up geophysical and geological investigations, the rupture parameters of the earthquake and the geometry of the fault are uncertain. Here we estimate the fault geometry, slip direction, and magnitude of the earthquake by modeling shoreline elevation change. The best fitting model geometry is a reverse fault with a shallow roof ramp consisting of at least two back thrusts. The best fitting rupture is a SW-NE oblique reverse slip with horizontal shortening of 15 m, rupture depth of 12.5 km, and magnitude Mw = 7.5.

Keywords: shoreline uplift, roof ramp, Seattle fault, shoreline angle, paleogeodesy.

INTRODUCTION

Co-seismically uplifted or subsided shorelines may provide paleogeodetic markers of large prehistoric earthquakes (Lajoie, 1986). Where precise measurements can be made, coastal uplift and subsidence can be modeled to infer fault slip parameters and even track inter-seismic movement (Natawidjaja et al., 2004; Shennan and Hamilton, 2006). Most previous analyses of abrupt elevation changes were focused on ruptures of plate interfaces in convergent margins (e.g., Ota and Yamaguchi, 2004). Such analyses are particularly useful in areas where large earthquakes have never been recorded with instruments. Abruptly raised shorelines ca. A.D. 900–930 (Bucknam et al., 1992; Sherrod, 2001; Fig. 1) and tsunami deposits at several sites between Seattle and Whidbey Island, Washington, United States (Atwater and Moore, 1992) were interpreted to have been generated by a large earthquake on the Seattle fault. No other large earthquakes have been documented on the fault since the retreat of glaciers ~15 ka, but smaller events took place between 2.5 and 1 ka (Nelson et al., 2003a). The Seattle fault is considered a major seismic hazard to the Seattle urban area because of its location and shallow rupture depth. The Seattle fault, a forearc fault with a total reverse throw of several kilometers, extends ~60–65 km in an east-west direction across the Puget Lowlands (Blakely et al., 2002), and separates sedimentary rocks of the subsurface Seattle Basin to the north from volcanic rocks of the Seattle uplift to the south (Johnson et al., 1994). Outcrops of basin-fill and sub-basin rocks along the surface projection of the fault on Bainbridge Island are tilted more than 70° (Fulmer, 1975). Surface exposures of the fault are either largely obscured by dense forest and thick glacial deposits (e.g., Nelson et al., 2003a), or are missing because fault rupture did not break the surface.

A variety of configurations and dips, ranging from 20° to 70°, have been proposed for the Seattle fault based on the interpretation of seismic reflection data, *P* wave velocity field, and the gravity field (Brocher et al., 2001; Johnson et al., 1999; Pratt et al., 1997; ten Brink et al., 2002). Because of their resolution, however, these data are only capable of providing long-term averages of the geometry and slip over geologic time. Focal mechanisms of small earthquakes in the vicinity of the fault do not provide a consistent rupture geometry and mechanism (Van Wagoner et al., 2002). Here we model the geometry of the fault during the A.D. 900–930 earthquake rupture by fitting the vertical displacement predicted by our model to the measured shoreline elevation change of Puget Sound. We use a dislocation model in a three-dimensional elastic model (Toda et al., 1998), an approach commonly applied to postseismic geodetic measurements of recent earthquakes (e.g., Lin et al., 1989). Puget Sound shoreline elevations cover the center of the 65-km-long-fault and are therefore expected to represent the displacement during the rupture.

DATA

The pre–A.D. 900 shoreline of Puget Sound is a horizontal datum that defines the pattern of vertical deformation produced by the earthquake, and the pattern, in turn, provides clues to the geometry of the faulting. Prior to uplift, the shore platform extended from about high tide at the foot of the steep coastal bluffs to at least several meters below mean lower low water (MLLW). To estimate the amount of uplift, we measured the height of the uplifted shoreline above modern tidal levels. Modern tidal levels have a mean range of 2.3 m (National Oceanic & Atmospheric Administration [NOAA] Nautical chart 18445). We use the sharp break in slope between the landward edge of the terrace and the adjoining steep hill slope, known as the shoreline angle, to estimate (Hull, 1987) the elevation of the uplifted shoreline (Fig. 1; Data Repository Table DR1[1]). Where the modern platform in the study area is cut on bedrock and not covered by sediment, the shoreline angle commonly lies near mean higher high water (MHHW). More commonly, the upper part of the modern platform is a zone of accumulation of sand and gravel, and the shoreline angle lies slightly above MHHW, typically marking the approximate upper limit of storm deposits (Hull, 1987).

Elevations of the shoreline angle were measured by surveying its height relative to a high or low tide (Fig. 1A). The measurements were referred to a known tidal datum using the observed level of the same tides at the Seattle tidal reference station, corrected to the nearest subordinate station. Because all measurement sites are within several ki-

[1]GSA Data Repository item 2006110, alternative models, sensitivity tests, and a table of observations, is available online at www.geosociety.org/pubs/ft2006.htm, or on request from editing@geosociety.org or Documents Secretary, GSA, P.O. Box 9140, Boulder, CO 80301, USA.

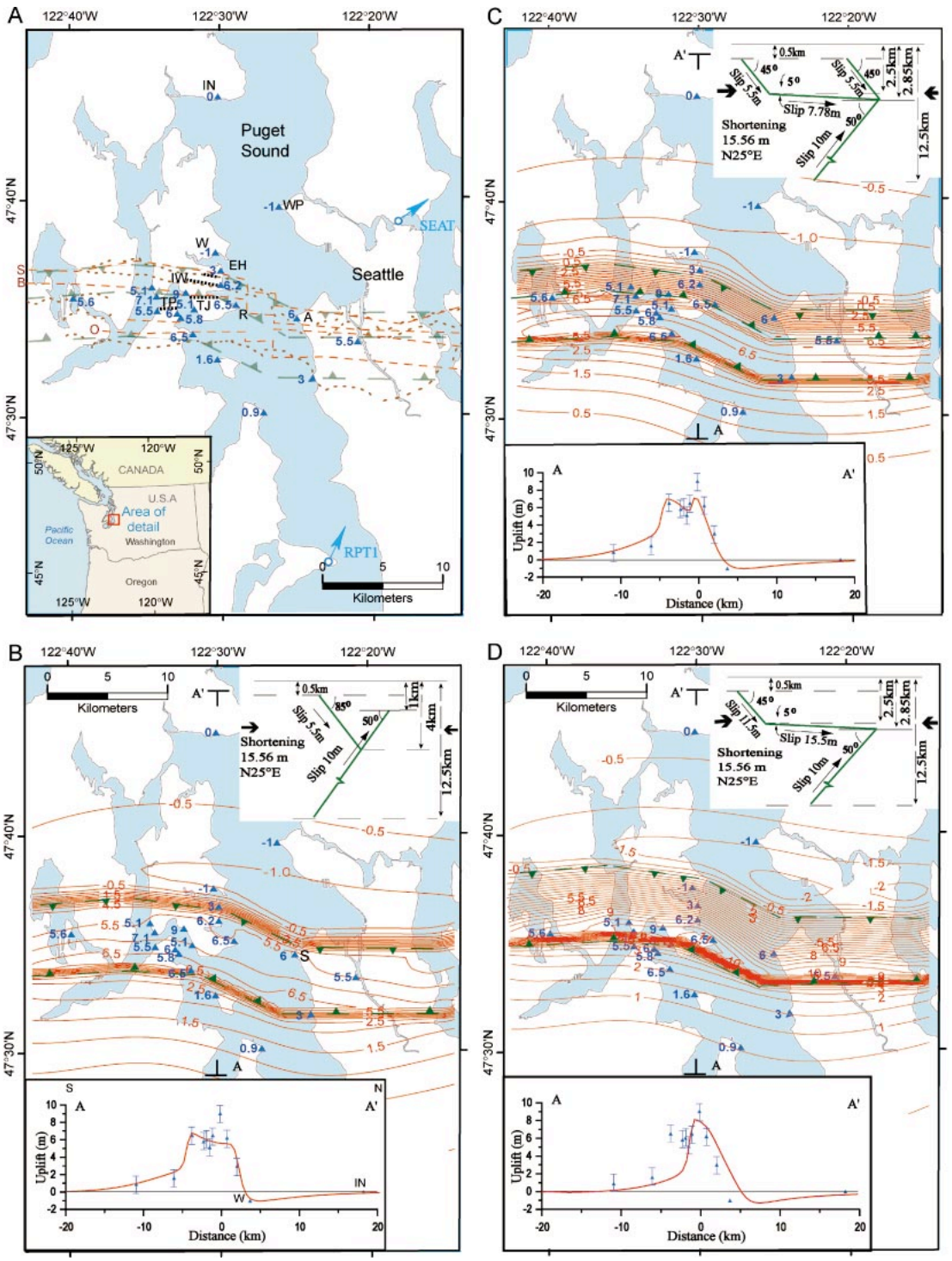

Figure 1. A: Observed shoreline uplift and subsidence as a result of the A.D. 900–930 earthquake (blue triangles). Locations are listed in Table DR1 (see footnote 1). Blue arrows are velocity vectors from global positioning system (GPS) stations near the Seattle fault relative to stable North America (Miller et al., 2001). Transparent green barbed lines are model faults in B, and C, projected vertically to the surface. Dashed red lines are locations of inferred Seattle (S), Blakely Harbor (B) and Orchard Point (O) faults from seismic reflection data (Johnson et al., 1999). Dotted brown lines are magnetization boundaries (Blakely et al., 2002). Dotted black lines are Toe Jam Hill (TJ), Waterman Point (TP), and Islandwood (IW) fault scarps from Lidar. A—Alki Point, EH—Eagle Harbor, IN—Indianola, R—Restoration Point, WP—West Point, W—Winslow. The 9 m observed uplift point includes uplift from an older event plus 3–4 m uplift from the earthquake 1100 yr ago (H. Kelsey, 2005, personal commun.). B–D: Calculated vertical elevation changes (red contours) for (B) wedge model geometry, (C) preferred roof thrust geometry, and (D) geometry and deformation front suggested by Brocher et al. (2004). Green barbed lines are model faults projected vertically to the surface. Upper-right corner insets show cross sections of these geometries (not to scale), and slip on the faults. Lower-left corner insets show cross-section A-A′ along longitude 122.5°W, with observations (blue triangles) and error bars of ± 1 m projected onto the model cross section (red line).

lometers of a subordinate tidal station, our geodetic surveys relative to local MHHW are probably accurate to within a few centimeters. Additional shoreline angle elevations (not shown) from Lidar surveys at sites in southern Bainbridge Island that appear free of post-uplift deposition or erosion agree with the elevations of land-based surveys. Modern shoreline angles, where they are cut on bedrock, are commonly at MHHW ± 0.7 m. Where sand and gravel are abundant, the shoreline angle is commonly ~0.5–1.0 m above MHHW. Hence, a conservative error in the difference between pre-uplift and modern tidal levels at each measurement site is about ± 1 m.

The elevation of the raised marine terraces along the Seattle fault probably contains components of postseismic tectonic deformation and sea-level change, which are difficult to quantify. For example, repeated measurements up to 4 yr after the 1993 Coalinga (California) earthquake indicate that the magnitude of postseismic deformation there is ~20% of the coseismic deformation (Stein and Ekstrom, 1992). Relative sea level in the Puget Sound rose no more than 1 m in the past 1000 yr (Eronen et al., 1987).

In comparison with the meters of uplift, subsidence on the north side of the Seattle fault was small. Elevation-sensitive salt marsh plants on a marsh surface at Winslow (see Figure 1A for location) changed from a fresh or fresh-brackish marsh to a salt marsh 1000 yr ago (Bucknam et al., 1992). The subsidence was probably less than 1 m. Subsidence in West Point probably did not exceed 1–1.5 m (B. Atwater,

2001, personal commun.), and no subsidence or uplift is documented near Indianola (B. Sherrod, 2001, personal commun.).

MODELING RUPTURE GEOMETRY

The uplift above the Seattle fault is a narrow (7 km) high of almost constant amplitude uplift (6–7 m), which abruptly decreases to ~1/6 of its value over 3 km to the south and continues to decrease gradually southward (bottom inset in Fig. 1B). To the north, the uplift changes abruptly to subsidence. We previously (ten Brink et al., 2002) showed that the narrow uplift zone cannot be fit with a single or multiple south-dipping reverse faults, as previously suggested (Calvert et al., 2001; Johnson et al., 1994). Instead, a more complex near-surface fault geometry with antithetic faults is required to fit the uplift shape. Two classes of fault geometries are investigated here, a reverse fault with a secondary antithetic thrust (the wedge model), and a roof thrust. The surface location of the modeled faults follows the Toe Jam Hill fault (Fig. 1A), identified in Lidar topography and in excavations, and the inferred fault traces from potential field data (Fig. 1). The faults in the model were divided into five linear segments to mimic the curved trace of the Seattle fault, and the results are linear superposition of displacement on all the segments. A regional shortening direction of N25°E was assumed following the global positioning system (GPS) vectors of most of the Puget Lowland stations relative to stable North America (Miller et al., 2001). The rake on each segment was varied as a function of the strike of the segment. A regional shortening direction of N54°E, as inferred from GPS station SEAT, could not be ruled out because of the limited spatial distribution of shoreline uplift data (Figure DR1A; see footnote 1). The N54°E regional shortening direction should produce a significant left-lateral component to the rupture. Earthquake focal mechanisms along the Seattle fault show predominantly oblique reverse slip and left-lateral strike slip (Van Wagoner et al., 2002).

The modeled primary reverse fault has the same geometry in both the wedge model and the roof-thrust model. It extends to a depth of 12.5 km and dips 50° to the south. As shown in the sensitivity models (Data Repository; see footnote 1), the dip is constrained by the subsidence north of the fault, where there are only three subsidence observations. The absence of subsidence near Indianola (Fig. 1A), and the small amplitude of subsidence at Winslow (Fig. 1A) immediately north of the surface trace of the Seattle fault, constrain the dip of the fault to 50° ± 5°. However, this model does not fit the subsidence at West Point on the east side of Puget Sound as well, whose magnitude is larger than that at Winslow. A better fit for the subsidence at West Point could be obtained by following Brocher et al.'s (2004) suggestion of locating the tip of the Seattle fault 2–3 km north of the deformation front. However, locating the fault tip north of Winslow results in uplift at Winslow, instead of the observed subsidence there, and higher uplift than observed along the southern shore of Eagle Harbor (Fig. 1D, or shifting the model contours northward by 3 km in Figures 1B and 1C). Hence, the steep gradient from subsidence in Winslow to uplift farther south determines not only the fault dip, but also the location of the fault tip near the inferred deformation front.

The wedge model (Fig. 1A) is perhaps the simplest geometry that will create a narrow zone of uplift (ten Brink et al., 2002). The surface projection of the back thrust in this model is constrained by the location of the abrupt drop-off at the south end of the narrow high-amplitude uplift. This location corresponds to the inferred Orchard Point Fault (Fig. 1A). The dip of the back thrust is constrained by the slope of the uplift, as defined by the two points south of the drop-off at 45° ± 10°. This model is capable of producing the observed sharp frontal gradient from uplift to subsidence above the primary fault, and a sharp backward drop above the synthetic fault, provided these faults extend to within 0.5–1 km of the surface. The junction between the primary and secondary faults at ~4 km is constrained by the dip of the faults and the location of their surface projection.

There are, however, two problems with the wedge geometry. First, it does not include the observed secondary antithetic thrust faults (the Toe Jam Hill fault—Bucknam et al., 1999; Nelson et al., 2003a; Waterman Point—Nelson et al., 2003b; and the Islandwood scarp—B. Sherrod, 2005, personal commun.), or the inferred Blakely Harbor fault (Johnson et al., 1999; Blakely et al., 2002). Second, shortening is not partitioned between the primary and secondary faults. Instead, the full 10 m of slip on the primary fault extends all the way to the surface, and an arbitrary slip of 5.5 m is set for the secondary slip. This implies that the primary and secondary faults could not have slipped during the same earthquake. A poor fit to the data is found when we attempt to divide the shortening at shallow levels between the primary and secondary faults (Figure DR1B; see footnote 1).

The geometry of the roof thrust model (Fig. 1B) is observed in many convergent settings (Brocher et al., 2004, and references therein) and is characterized by shallow faults, which can have different dips and directions than the primary deeper fault. A ramp at a depth of ~3 km fits our observations (Fig. 1C), whereas a deeper roof thrust system (Brocher et al., 2004) will produce a broader uplift with gentler gradients to the north and south. A frontal backthrust rising from the tip of the wedge and propagating to the near surface is needed to mimic the steep frontal gradient from uplift to subsidence. The modeled frontal back thrust is located between the Toe Jam Hill fault and the Islandwood scarp. Without the frontal back thrust (Brocher et al., 2004), the model does not fit the observed uplift, because it produces a gradual frontal surface gradient that reaches its maximum uplift south of Restoration Point (Fig. 1D).

The roof thrust model generates a slightly gentler frontal slope than the wedge model because the shallow frontal thrust dips northward, but the frontal elevation is higher (compare the cross sections in the insets of Figures 1B and 1C). The horizontal shortening in the roof thrust model can be distributed proportionally as slip on all faults, implying that, unlike the wedge model, all the components of the faults could have ruptured simultaneously. The roof thrust model is likely a simplification of a more complex geometry with more fault splays that are exposed in a few locations. This geometry is too complex to be modeled with our model resolution and with the available distribution of observations. For example, extending modeled fault slip to the surface, as observed in the Toe Jam Hill fault (Nelson et al., 2003a), generates high local surface amplitudes. Increasing the number of antithetic faults to fit the observed slip of 2.1–2.8 m on the Toe Jam Hill fault (Nelson et al., 2003a) does not change the uplift pattern, but requires a finer numerical grid. The model suggests, however, that the roof thrust must accommodate more horizontal shortening than is accounted for by slip on exposed faults (Nelson et al., 2003a).

RUPTURE PARAMETERS

Both the wedge and the roof thrust models fit the uplift and subsidence observations best with a 50° south-dipping reverse fault extending to a depth of 12.5 km, and with secondary back thrusts extending to within 0.5–1 km of the surface and occasionally breaking the surface. The model suggests step folds above the buried primary fault (ten Brink et al., 2002), like those observed (Fulmer, 1975; B. Sherrod, 2005, personal commun.). The location of the primary and secondary faults matches the inferred faults from magnetic data and the Toe Jam Hill fault scarp identified on Lidar. The shortening direction for both models is SW-NE, in agreement with the relative motion of GPS stations in the Puget Lowland and with earthquake focal mechanisms. The amount of horizontal shortening necessary to produce the observed uplift is 15.6 m, assuming that all the observed uplift was due to coseismic slip, and ignoring up to 1 m of sea-level rise during

the past 1100 yr. We assume that the amounts of postseismic slip, 20% of total slip, and sea-level rise (<1 m) since the A.D. 900–930 earthquake are roughly similar and so they cancel each other. Dividing 15.6 m by ~14 k.y. (the time between the last glacial retreat and the late Holocene) gives an average shortening of ~1.1 mm/yr, a similar value to the N-S shortening observed across the Seattle fault from GPS (Miller et al., 2001). The wedge model predicts additional shortening on the secondary fault, whereas the roof thrust model predicts simultaneous rupture on all the faults.

The calculated moment for the wedge model is 2.72×10^{27} dyne-cm, and for the roof thrust model it is 2.64×10^{27} dyne-cm. The calculated earthquake magnitude for both models is Mw = 7.55, slightly less than Pratt et al.'s (1997) estimate from an empirical fault area-magnitude relation. The calculated moment is based on modeling the 35-km-long central segment of the fault, but the seismic moment could be higher if we include the non-modeled fault continuations to the east and west. On the other hand, the actual slip distribution during an earthquake is almost never uniform, whereas we assumed uniform slip in all the modeled fault segments.

This analysis demonstrates the utility of shoreline elevation changes to the study of earthquakes unrecorded by instruments. It highlights the need for additional paleogeodetic data around the Seattle fault, particularly additional subsidence data north of the fault, and uplift data farther south of the fault, to better constrain the primary fault parameters. It also highlights the hazard to the Seattle metropolitan area from near-surface focused deformation and uplift by a roof thrust or a wedge complex during an earthquake.

ACKNOWLEDGMENTS

We gratefully acknowledge discussions with Brian Atwater, Brian Sherrod, Ross Stein, and Tom Brocher, and thorough and helpful reviews by H. Kelsey, A. Nelson, B. Sherrod, T. Brocher, and an anonymous reviewer.

REFERENCES CITED

Atwater, B.F., and Moore, A.L., 1992, A tsunami about 1000 years ago in Puget Sound, Washington: Science, v. 258, p. 1614–1617.

Blakely, R.J., Wells, R.E., Weaver, C.S., and Johnson, S.Y., 2002, Location, structure, and seismicity of the Seattle fault zone, Washington; Evidence from aeromagnetic anomalies, geologic mapping, and seismic-reflection data: Geological Society of America Bulletin, v. 114, p. 169–177.

Brocher, T.M., Parsons, T., Blakely, R.J., Christensen, N.I., Fisher, M.A., Wells, R.E., and the Seismic Hazards Investigations in Puget Sound (SHIPS) Working Group, 2001, Upper crustal structure in Puget Lowland, Washington: Results from the 1998 Seismic Hazards Investigation in Puget Sound: Journal of Geophysical Research, v. 106, p. 13,541–13,564.

Brocher, T.M., Blakely, R.J., and Wells, R.E., 2004, Interpretation of the Seattle Uplift, Washington, as a passive-roof duplex: Bulletin of the Seismological Society of America, v. 94, p. 1379–1401.

Bucknam, R.C., Hemphill-Haley, E., and Leopold, E.B., 1992, Abrupt uplift within the past 1700 years at southern Puget Sound, Washington: Science, v. 258, p. 1611–1614.

Bucknam, R.C., Sherrod, B.L., and Elfendahl, G., 1999, A fault scarp of probable Holocene age in the Seattle fault zone, Bainbridge Island, Washington: Seismological Research Letters, v. 70, p. 233.

Calvert, A.J., Fisher, M.A., and the Seismic Hazards Investigations in Puget Sound (SHIPS) Working Group, 2001, Imaging the Seattle fault zone with high-resolution seismic tomography: Geophysical Research Letters, v. 28, p. 2337–2340.

Eronen, M., Kankainen, T., and Tsukada, M., 1987, Late Holocene sea-level record in a core from the Puget Lowland: Quaternary Research, v. 27, p. 147–159.

Fulmer, C.V., 1975, Stratigraphy and paleontology of the type Blakely and Blakely Harbor formations, *in* Weaver, D.W., et al., eds., Paleogene symposium and selected technical papers, Conference on future energy horizons of the Pacific Coast: Long Beach, California, Pacific Section, American Association of Petroleum Geologists, p. 210–271.

Hull, A.G., 1987, A late Holocene marine terrace on the Kidnappers Coast, North Island, New Zealand; Some implications for shore platform development processes and uplift mechanism: Quaternary Research, v. 28, p. 183–195.

Johnson, S.Y., Potter, C.J., and Armentrout, J.M., 1994, Origin and evolution of the Seattle fault and Seattle basin, Washington: Geology, v. 22, p. 71–74.

Johnson, S.Y., Dadisman, S.V., Childs, J.R., and Stanley, W.D., 1999, Active tectonics of the Seattle fault and central Puget Sound, Washington; Implications for earthquake hazards: Geological Society of America Bulletin, v. 111, p. 1042–1053.

Lajoie, K.R., 1986, Coastal tectonics, *in* Wallace, R.E., ed., Active tectonics: Washington, D.C., National Academic Press, p. 95–124.

Lin, J., Stein, R.S., and Anonymous, 1989, Coseismic folding, earthquake recurrence, and the 1987 source mechanism at Whittier Narrows, Los Angeles Basin, California: Journal of Geophysical Research, v. 94, p. 9614–9632.

Miller, M.M., Johnson, D.J., Rubin, C.M., Dragert, H., Wang, K., Qamar, A., and Goldfinger, C., 2001, GPS-determination of along-strike variation in Cascadia margin kinematics; Implications for relative plate motion, subduction zone coupling, and permanent deformation: Tectonics, v. 20, p. 161–176.

Natawidjaja, D.H., Sieh, K., Ward, S.N., Cheng, H., Edwards, R.L., Galetzka, J., and Suwargadi, B.W., 2004, Paleogeodetic records of seismic and aseismic subduction from central Sumatran microatolls, Indonesia: Journal of Geophysical Research, v. 109, no. 4, p. 34.

Nelson, A.R., Johnson, S.Y., Kelsey, H.M., Wells, R.E., Sherrod, B.L., Pezzopane, S.K., Bradley, L.-A., Koehler, R.D., III, and Bucknam, R.C., 2003a, Late Holocene earthquakes on the Toe Jam Hill fault, Seattle fault zone, Bainbridge Island, Washington: Geological Society of America Bulletin, v. 115, p. 1388–1403.

Nelson, A.R., Johnson, S.Y., Kelsey, H.M., Sherrod, B.L., Wells, R.E., Okumura, K., Bradley, L.-A., Bogar, R., and Personius, S.F., 2003b, Field and laboratory data from an earthquake history study of the Waterman Point Fault, Kitsap County, Washington: U.S. Geological Survey Miscellaneous Field Studies MF-2423, 1 sheet.

Ota, Y., and Yamaguchi, M., 2004, Holocene coastal uplift in the western Pacific Rim in the context of late Quaternary uplift: Quaternary International, v. 120, p. 105–117.

Pratt, T.L., Johnson, S.Y., Potter, C.J., Stephenson, W.J., and Finn, C.A., 1997, Seismic reflection images beneath Puget Sound, western Washington State; The Puget Lowland thrust sheet hypothesis: Journal of Geophysical Research, v. 102, p. 27,469–27,489.

Shennan, I., and Hamilton, S.L., 2006, Coseismic and pre-seismic subsidence associated with great earthquakes in Alaska: Quaternary Science Reviews, v. 24, p. 1–8.

Sherrod, B.L., 2001, Evidence for earthquake-induced subsidence about 1100 yr ago in coastal marshes of southern Puget Sound, Washington: Geological Society of America Bulletin, v. 113, p. 1299–1311.

Stein, R.S., and Ekstrom, G., 1992, Seismicity and geometry of a 110-km-long blind thrust fault; 2, Synthesis of the 1982–1985 California earthquake sequence: Journal of Geophysical Research, v. 97, p. 4865–4883.

ten Brink, U.S., Molzer, P.C., Fisher, M.A., Blakely, R.J., Bucknam, R.C., Parsons, T., Crosson, R.S., and Creager, K.C., 2002, Subsurface geometry and evolution of the Seattle fault zone and the Seattle Basin, Washington: Bulletin of the Seismological Society of America, v. 92, p. 1737–1753.

Toda, S., Stein, R.S., Reasenberg, P.A., Dieterich, J.H., and Yoshida, A., 1998, Stress transferred by the 1995 Mw=6.9 Kobe, Japan, shock: Effect on aftershocks and future earthquake probabilities: Journal of Geophysical Research, v. 103, p. 24,543–24,565.

Van Wagoner, T.M., Crosson, R.S., Creager, K.C., Medema, G., Preston, L., Symons, N.P., and Brocher, T.M., 2002, Crustal structure and relocated earthquakes in the Puget Lowland, Washington, from high-resolution seismic tomography: Journal of Geophysical Research, v. 107, no. 12, p. 23.

Manuscript received 28 August 2005
Revised manuscript received 4 January 2006
Manuscript accepted 14 February 2006

Printed in USA